Cytokine 84 (2016) 47–55

Contents lists available at ScienceDirect

Cytokine

journal homepage: www.journals.elsevier.com/cytokine

Cytotoxic effects induced by interferon-ω gene lipofection through ROS generation and mitochondrial membrane potential disruption in feline mammary carcinoma cells

Marcela Solange Villaverde [a], Alexandra Marisa Targovnik [b], María Victoria Miranda [b], Liliana María Elena Finocchiaro [a], Gerardo Claudio Glikin [a,*]

[a] Unidad de Transferencia Genética, Instituto de Oncología "Ángel H. Roffo", Universidad de Buenos Aires, Av. San Martín 5481, 1417 Buenos Aires, Argentina
[b] Instituto de Nanobiotecnología (NANOBIOTEC, CONICET-UBA), Cátedra de Microbiología Industrial y Biotecnología, Facultad de Farmacia y Bioquímica (UBA), Junín 956, 1113 Buenos Aires, Argentina

ARTICLE INFO

Article history:
Received 8 January 2016
Received in revised form 3 May 2016
Accepted 18 May 2016

Keywords:
Feline interferon-omega
Plasmid lipofection
ROS
Feline mammary carcinoma

ABSTRACT

Progress in comparative oncology promises advances in clinical cancer treatments for both companion animals and humans. In this context, feline mammary carcinoma (FMC) cells have been proposed as a suitable model to study human breast cancer. Based on our previous data about the advantages of using type I interferon gene therapy over the respective recombinant DNA derived protein, the present work explored the effects of feline interferon-ω gene (fIFNω) transfer on FMC cells. Three different cell variants derived from a single spontaneous highly aggressive FMC tumor were successfully established and characterized. Lipofection of the fIFNω gene displayed a significant cytotoxic effect on the three cell variants. The extent of the response was proportional to ROS generation, mitochondrial membrane potential disruption and calcium uptake. Moreover, a lower sensitivity to the treatment correlated with a higher malignant phenotype. Our results suggest that fIFNω lipofection could offer an alternative approach in veterinary oncology with equal or superior outcome and with less adverse effects than recombinant fIFNω therapy.

1. Introduction

Some types of human cancer are very similar to the corresponding disease in companion animals. Progress made studying these cancers can be very helpful for pets as well as it can lead to advances in the treatment of human patients [1]. Feline mammary carcinomas (FMC) are among the most common feline tumors and represent an important cause of mortality. The incidence and morbidity of these tumors are very high because their biological behavior is characterized by a rapid growth, high proliferation rates, and the ability to metastasize to regional lymph nodes and distant organs [19]. Mammary tumors in cats are particularly frequent and have been proposed as spontaneous models of breast cancer, but they might be suitable only to study certain molecular subtypes Compared to humans, cats tend to have a high percentage of mammary tumors that are hormone receptor-negative. Therefore, they could be useful as models to study hormone-refractory breast cancer [7,26]. The basal-like properties of FMC offer another avenue for future research in the field of comparative oncology [13]. As it was observed in humans, the expression of the HER2 oncogene in feline mammary tissues correlates with the clinical course of the disease [19]. Immunotherapy with recombinant human interferon-α (rhIFNα) was approved for melanoma, leukemia and lymphoma and is under study in clinical trials for some other malignancies [34]. Recombinant feline interferon omega (rfIFNω, Virbac®) was approved for use against selected viral diseases in cats and dogs [3] and displayed *in vitro* growth inhibition activities on various canine and feline tumor cell lines [22,28]. While other cytokines were assayed for feline fibrosarcoma immunogene therapy [11], we have previously demonstrated that hIFNβ gene lipofection may constitute an approach that produces an effect equal to or superior than that of high doses of the exogenously applied rhIFNβ protein [30]. Thus, gene transfer would allow taking advantage of the effect of type I IFNs without undesirable side effects.

In the present study, we evaluated for the first time the effects of fINFω gene lipofection on different variants of FMC cells, demonstrating the therapeutic potential of this approach. Besides, we suggest the involvement of ROS related mechanisms in these effects. On the other hand, we found differentiation state related

* Corresponding author at: Unidad de Transferencia Genética, Instituto de Oncología "A.H. Roffo" – UBA, Av. San Martín 5481, 1417 Buenos Aires, Argentina.
E-mail address: gglikin@bg.fcen.uba.ar (G.C. Glikin).

http://dx.doi.org/10.1016/j.cyto.2016.05.018
1043-4666/

changes in the cell variants and the correlation of higher aggressiveness with lower sensitivity to fINFω treatments.

2. Materials and methods

2.1. Cell cultures

FMC cells were established from an infiltrating mammary adenocarcinoma. Briefly, a mammary tumor from a 10-year-old female Siamese cat was resected. The tumor was histologically classified as a cribriform type. Tumor cells were mechanically disrupted. The resulting cell suspension was centrifuged, washed with PBS and cultured as monolayers at 37 °C in a humidified atmosphere of 95% air and 5% CO_2 with DMEM/F12 medium (Invitrogen, Carlsbad, CA, USA) containing 10% FBS (Invitrogen), 10 mM HEPES (pH 7.4) and antibiotics. Serial passages were made by trypsinization (0.25% trypsin and 0.02% EDTA in PBS) of subconfluent monolayers. Passages from 20 to 30 were arbitrarily named *AlRB*. Passages from 60 to 70 were named *AlRA*. Finally, the *AlRA10* variant was obtained by continuous exposure of *AlRB* cells to rfIFNω (10 IU/ml) until reaching passage number 60. For doubling time estimation using GraphPad Prism 6 software (GraphPad Software Inc., USA), FMC cells were trypsinized and 5×10^4 cells were plated in duplicate in 35-mm plates and cultured in normal conditions. After trypan blue dying, cells were daily counted in a Neubauer chamber.

2.2. Plasmids

Plasmids psCMVbgal (6.8 kb) and psCMVfIFNω (3.9 kb) carry respectively, *Escherichia coli* β-galactosidase gene (3.5 kb), feline IFNω (0.6 kb) in the polylinker site of psCMV (3.3 kb), downstream of the CMV promoter and upstream of poly A sequences. The plasmids (bearing kanamycin resistance gene for selection in *E. coli*) were amplified, chromatographically purified and quality assessed as described [25]. Plasmid DNA for injection was resuspended to a final concentration of 2.0 mg/ml in sterile PBS.

2.3. Liposome preparation and lipofection efficiency assay

DC-Chol (3β[N-(N′,N′-dimethylaminoethane)-carbamoyl] cholesterol) and DMRIE (1,2-dimyristyl oxypropyl-3-dimethyl-hid roxyethylammonium bromide) were synthesized and kindly provided by BioSidus (Argentina). DOPE (1,2-dioleoyl-*sn*-glycero-3-phosphatidyl ethanolamine) was purchased from Sigma-Aldrich de Argentina (Argentina). Liposomes were prepared at lipid/co-lipid molar ratios of 3:2 (DC-Chol:DOPE) or 1:1 (DMRIE:DOPE) by sonication as described [25]. Optimal lipid mixtures were determined for every cell lines.

In most experiments, cells were seeded into 12-well plates at a density of $3–6 \times 10^4$ cells/cm^2 and were allowed to adhere overnight. Monolayers were exposed to lipoplexes (0.5 μg plasmid DNA/cm^2 and 1 μl liposome/cm^2) from 2 to 5 h in a serum-free medium. Then the lipofection medium was replaced with fresh complete medium.

Transfection rates were checked 24 h after lipofection by β-galactosidase staining with 5-bromo-4-chloro-3-indolyl b-D-galactopyranoside (X-GAL, Sigma) to ensure that they were comparable in different experiments and counted using an inverted phase contrast microscope [25].

2.4. Cloning efficiency in soft agar

Dispersed cells were resuspended in 0.25% agar in culture medium at 1×10^4 cells/ml and layered on top of 0.5% agar in culture medium. Three weeks after initiating cultures, colonies were counted.

2.5. Immunocytochemistry

Cells were cultured for 48 h in normal conditions on a glass slides. Then, cells were washed, fixed with ethanol, dried, rehydrated and incubated with the corresponding primary mouse antibody against estrogen receptor (ER) (1:500), progesterone receptor (PR) (1:500), human epidermal growth factor receptor 2, (HER2, 1:500), vimentin (1:100), cytokeratin 5 (CK5; 1:500), cytokeratin 18 (CK18; 1:200), E-cadherin (E-cad, 1:500) and alpha smooth muscle actin (α-SMA; 1:500) overnight at 4 °C. After rinsing, cells were incubated with a 1:200 dilution of peroxidase-conjugated anti-mouse IgG (Sigma, St. Louis, MO, USA) at room temperature for 2 h. Cells were counterstained with hematoxylin and eosin.

2.6. fIFNω treatment

FMC cells were plated at a density of 5×10^4 cells/cm^2 and 24 h later either lipofected with the βgal or fIFNω gene (as previously described in [30]) or treated with exogenous rfIFNω (1–10,000 IU/ml). After 5 days of treatment, cell viability was quantified with the acid phosphatase assay (APH) [9]. The percentage of cell survival was calculated from the ratio of the absorbance between lipofected and untreated control cells. Gene transfer efficiency was determined by staining βgal-lipofected cells with X-gal (Sigma) and counted with an inverted phase contrast microscope.

2.7. fIFNω antiviral biological activity

The supernatants of control (untreated), βgal- and fIFNω-lipofected cells were collected (24 h after lipofection) and assayed for fIFNω by a biological method involving VSV infected CRFK cells as described [27].

2.8. Cell cycle analysis

Control and fIFNω-treated cells were harvested after 48 h or 96 h of treatment, fixed in 70% (v/v) ethanol at −20 °C for 1 h, treated with RNAse and stained with 10 μg/ml propidium iodide (Sigma) for 30 min and analyzed by flow cytometry in a Becton Dickinson FACScan (Franklin Lakes, NJ), with collection and analysis of data performed using Becton Dickinson CELLQuest software.

2.9. Membrane integrity analysis

Propidium iodide (PI) enters the cells only if there is a loss of membrane integrity. Control and fIFNω-treated cells were harvested after 48 h of treatment, incubated for 5 min with 5 mg/ml PI and analyzed by flow cytometry as described above.

2.10. Reactive oxygen species (ROS) detection

Control and fIFNω-treated cells were harvested after 48 h of treatment. Then, the cells were rinsed, washed with PBS and incubated with 0.5 μM H_2DCFDA (Invitrogen), a cell-permeable non-fluorescent dye that in the presence of intracellular oxidants is converted in fluorescent DCF [6]. After 20 min, normal culture conditions were re-established and the cellular fluorescence intensity was analyzed by flow cytometry as described above.

2.11. Mitochondrial membrane potential ($\Delta\psi$) measurement

Cells were harvested after 48 h of treatment, washed with PBS and incubated with 10 μg/ml of JC-1 (Invitrogen), a cationic dye that is accumulated in mitochondria according to membrane potential. At low concentrations, the probe is present in monomeric form, with green fluorescence emission (525 nm), but at higher concentrations it forms J-aggregates after accumulation in mitochondria, with red fluorescence emission (590 nm). After 20 min, normal culture conditions were re-established and the cellular fluorescence intensity was analyzed by flow cytometry as described above. Mitochondrial depolarization was indicated by a decrease in the red/green fluorescence intensity ratio.

2.12. Ca^{2+} uptake analysis

Control and flFNω-treated cells were harvested after 72 h of treatment, washed with PBS and incubated with Fura 2-AM (0.2 μM; Invitrogen), a non-fluorescent cell-permeable dye that forms a fluorescent complex with calcium. After 20 min, normal

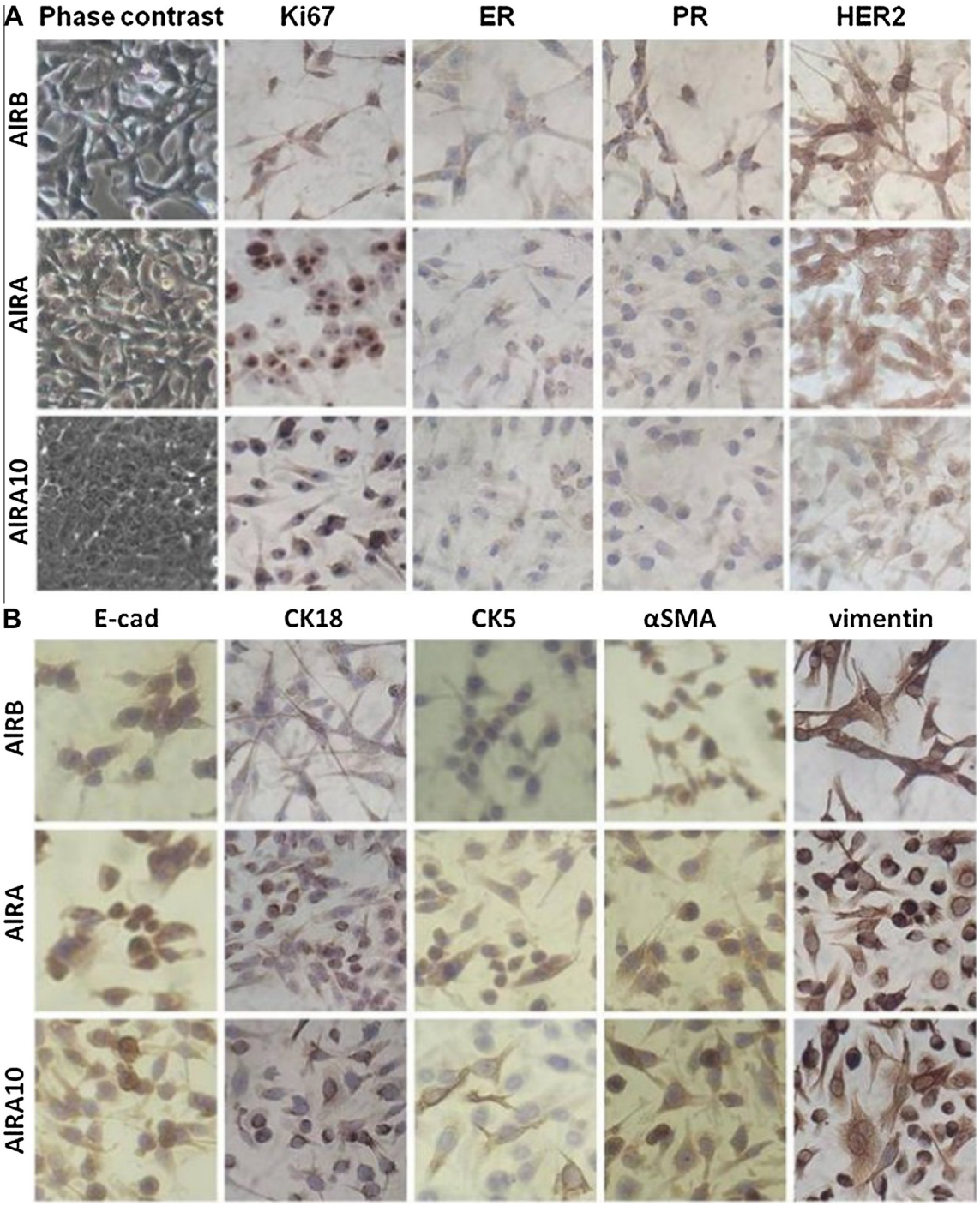

Fig. 1. (A) Characterization of FMC cells antigens. (B) Epithelial-mesenchymal transition markers. Ki67, estrogen receptor (ER), progesterone receptor (PR) and human epidermal growth factor receptor 2 (HER2), E-cadherin (E-cad), 18-cytokeratin (CK18) 5-cytokeratin (CK5), alpha-smooth muscle actin (αSMA) and vimentin expression were detected by immunocytochemistry using specific antibodies as described in Section 2 and photographed (200×).

culture conditions were re-established and Cl_2Ca was added (250 μM) immediately before evaluation by flow cytometry as described above.

2.13. Statistical analysis

Differences between groups were analyzed with one- or two-way ANOVA followed by multiple comparisons Tukey's test. $p < 0.05$ was established as significant. Analyses were made using INFOSTAT free edition and GraphPad Prism 6 software (GraphPad Software Inc., USA).

3. Results

3.1. Establishment and characterization of FMC cell lines

Although in the last few years feline mammary carcinoma (FMC) cells have been proposed as an interesting model to study human breast carcinoma by several authors [16,31], they are not yet commercially available. In the present work, three variants of FMC cells were successfully established from a single spontaneous mammary carcinoma culture named *Al*. The resected tumor was processed as described in Section 2.1.

Multiple passages of FMC cells (60–70) were performed to mimic the possible evolution of tumor cells during disease progression without treatment. Passages in the presence of rfIFNω were also made for the selection of cells resistant to fIFNω recreating the conditions of a chronic treatment. Drug resistance is a phenomenon that usually appears after long term treatments.

As displayed in phase contrast micrographs taken when cultures reached confluence (Fig. 1), *AlRB* and *AlRA* presented a network of elongated fibroblastic shaped cells, while *AlRA10* appeared more densely and tightly packed yielding more isometric cells. These differences were not evident in subconfluent cultures, as shown after immunocytochemistry staining.

Once reaching passage 20 (up to 30), early *Al* cells (named *AlRB*) displayed a fibroblastic shape and a disperse monolayer (Fig. 1A) that was easily detachable by trypsinization (Fig. 2A), probably as a sign of a lowly adherent phenotype or differences in the generated extracellular matrix. In line with these results, we found that *AlRB* was positive for the mesenchymal marker vimentin and negative for the epithelial marker E-cadherin (Fig. 1B). Taking into account its diagnostic relevance, we evaluated the hormone receptor and HER2 status (Fig. 1A). Interestingly, we found that *AlRB* was PR- and ER-negative and highly positive (3+) for the HER2 oncogene. These results are in partial agreement with previous reports [4,17,19,20], confirming that most feline mammary tumors are negative for hormone receptors.

In an attempt to mimic the growing tumor *in vivo*, we kept cells proliferating *in vitro* and after passage #30, FMC cells were separately cultured without or with rfINFω (10 IU/ml) and when reaching passages #60–70, respectively named *AlRA* and *AlRA10*. Both *AlRA* and *AlRA10* showed higher epithelial features than *AlRB* and were highly positive for vimentin, presenting subpopulations of E-cadherin-positive cells (Fig. 1). These results are consistent with a higher cell-to-cell and cell-substrate interactions and consistent with a 3-fold increase of *AlRA10* detachment time under trypsin treatment (Fig. 2A). *AlRA* and *AlRA10* were also more stained for the epithelial marker CK18 than *AlRB* (Fig. 1B). Interestingly, *AlRA10* presented a positive subpopulation for αSMA and CK5 (Fig. 1B) suggesting some basal-like features. The hormone receptor status did not change between variants. While *AlRA* presented a mild immunoreactivity, *AlRA10* was almost negative for HER2.

Duplication times were significantly shorter for *AlRA* and *AlRA10* than for *AlRB* (16 and 18 h respectively *vs.* 25 h, Fig. 2B). Accordingly, only 3–5% of *AlRB* nuclei were positive for the specific proliferation marker Ki67 whereas more than 50% of *AlRA* and *AlRA10* nuclei were so (Fig. 1A). In addition, *AlRA10* displayed a more aggressive phenotype by forming colonies in soft agar while *AlRB* and *AlRA* did not (Fig. 2C).

3.2. flFNω lipofection diminished survival of FMC cells

To evaluate the extent of antitumor activity displayed by fIFNω gene transfer on FMC cells, the three cell lines were lipofected with fIFNω gene or otherwise incubated with exogenously added rfIFNω (3000 IU/ml). After 5 days of treatment, cell survival was determined by the acid phosphatase activity test. *AlRB* cells were highly sensitive (Fig. 3A and B) to interferon with both strategies. In the case of the added protein, the magnitude of the response was concentration-dependent (Fig. 3A). While *AlRA* was mildly sensitive, *AlRA10* was not significantly sensitive to rfIFNω. Although the three FMC cell variants were sensitive to fIFNω-lipofection, the magnitude of the response varied significantly between them, the cell death rates being about 70% for *AlRB*, 50% for *AlRA* and 30% for *AlRA10* (Fig. 3B).

Remarkably, the three cell lines displayed equivalent lipofection efficiency (<2%) as assayed by β-galactosidase marker (data not shown). As previously reported, the antitumor activity of interferon gene transfer is significantly effective even with low lipofection efficiencies [30]. In addition, the production of fIFNω

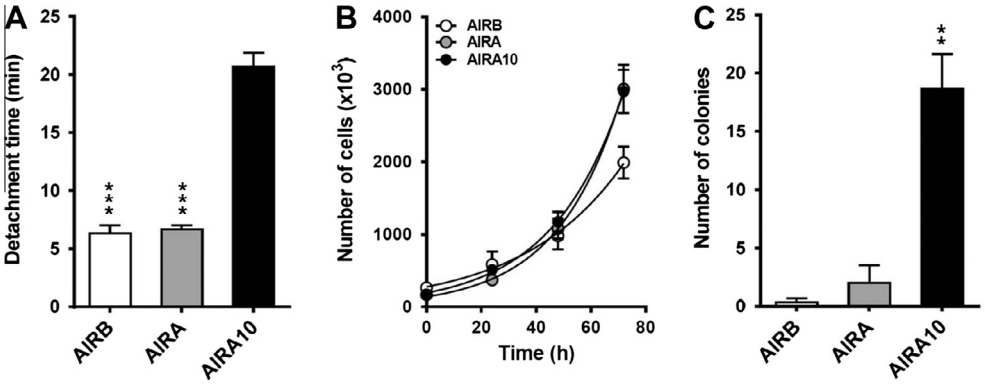

Fig. 2. (A) Trypsin driven detachment of FMC cells. Monolayer cultured cells were treated with trypsin and then observed under microscope every minute. (B) Cell growth curves. Total cell number was determined at 0, 24, 48 and 72 h after plating. (C) Cell growth in soft agar. Colonies were counted 3 weeks after plating. Results are expressed as means ± s.e.m of independent experiments ($n > 3$). $^{**}p < 0.01$; $^{***}p < 0.001$.

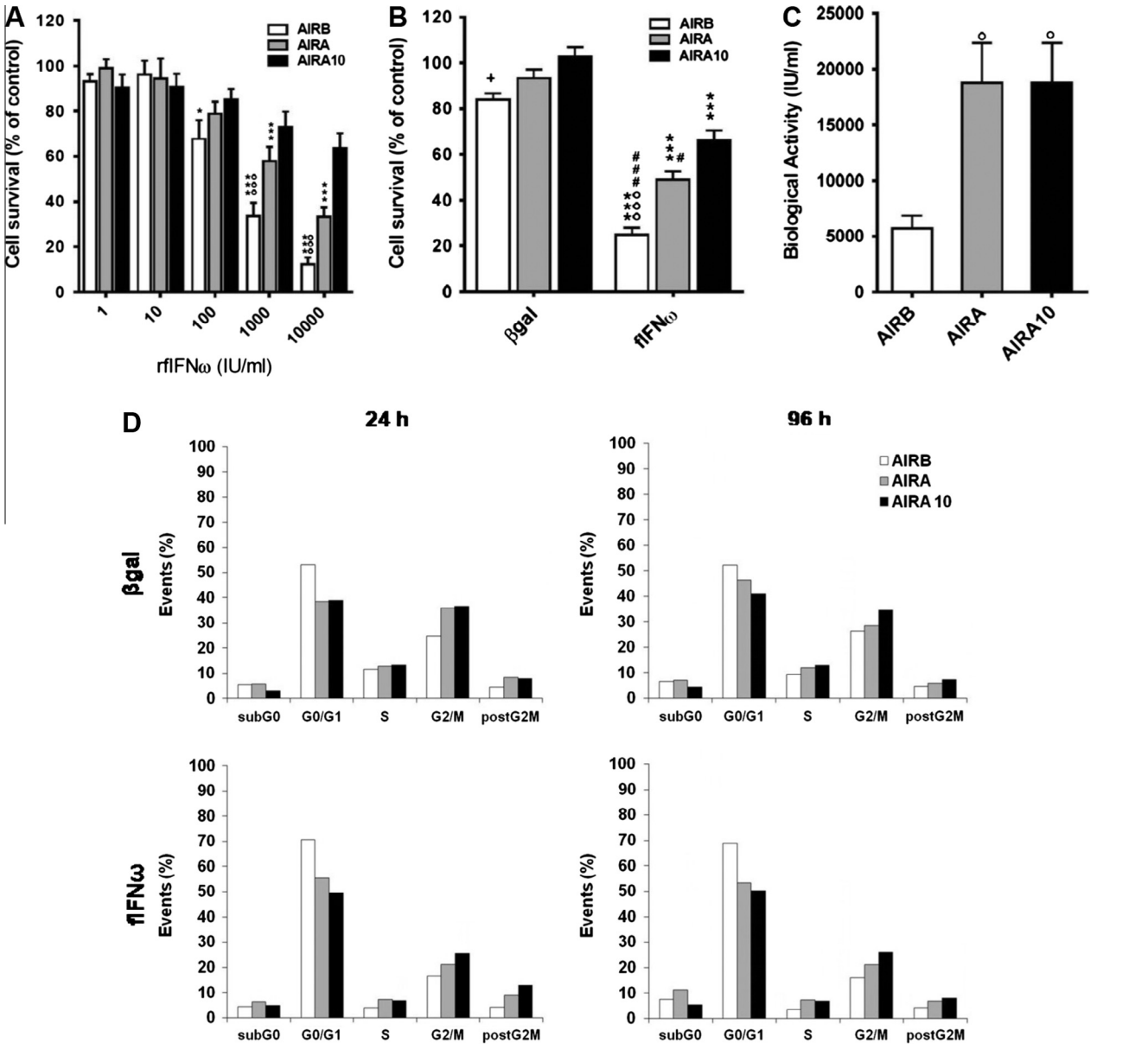

Fig. 3. Cytotoxic effects of fINFω transferred gene (A) or exogenously added rfINFω protein (B) on FMC cells. (A) Transiently βgal- or fINFω-lipofected cells were cultured as monolayers and cell viability was quantified by the APH assay on day 5 as described in Section 2. Results are expressed as means ± s.e.m of n > 9 independent experiments. (B) Cell monolayers were grown in the presence of increasing concentrations of rfINFω as indicated and cell viability was quantified by the APH assay on day 5. Results are expressed as percentage of viable cells with respect to the untreated control (100%) as means ± s.e.m; n > 9. (C) fINFω biological activity in supernatant media of treated cells. It was evaluated as described in Section 2. $^{***}p < 0.001$ with respect to 1 IU/ml or respect to βgal. $^{+}p < 0.05$ with respect to *AIRB*-βgal; $^{\circ}p < 0.05$ and $^{\circ\circ\circ}p < 0.001$ with respect to *AIRB* and $^{\#}p < 0.05$ with respect to *AIRA*. (D) Cell cycle analysis. βgal- or fINFω-lipofected cells were harvested after 48 h or 96 h of treatment, stained with PI and analyzed by a flow cytometry as described in Section 2.

protein by lipofected cells was confirmed by Western blot and immunocytochemistry (data not shown), and a biological activity test (Fig. 3C). *AIRA* and *AIRA10* supernatants presented significantly higher fIFNω biological activity as compared to *AIRB*. Therefore, differences in the magnitude of the response observed between variants were not due to a lack of protein production.

After fIFNω gene lipofection, none of the FMC cells presented a significantly modified cell cycle distribution pattern (compared to control βgal gene lipofection) despite their decreasing survivals (Fig. 3D). The higher percentage of *AIRA* and *AIRA10* cells in the DNA synthesis phase (S phase) and mitosis (G2/M) phase (Fig. 3D) was consistent with the higher growth rate observed in these variants as compared to AIRB.

3.3. *fIFNω treatment increased the fraction of apoptotic/necrotic cells in AIRB and AIRA*

Subsequently, we explored whether the cytotoxic effects of the fIFNω gene on the FMC variants were correlated with increased apoptotic/necrotic (A/N) events.

Viable cells are non-permeable for PI, while late A/N cells allow PI uptake because of membrane integrity loss. *AIRB*, *AIRA* and *AIRA10* cells were lipofected with the βgal or fIFNω gene or incubated with exogenously added rfIFNω (3000 IU/ml). After 48 h, cells were harvested and freshly stained (without fixation) with PI solution (5 μg/ml), and then analyzed by flow cytometry. In agreement with the survival results, *AIRB* presented the highest

percentage of A/N cells for both treatments at the evaluated time. In *AlRB* and *AlRA* variants, this percentage was significantly higher for flFNω gene transfer than for rflFNω protein addition (Fig. 4). After treatment with the flFNω gene or rflFNω protein, the less sensitive *AlRA10* did not display any significantly increase of A/N cells at the tested time (Fig. 4A). As expected, PI permeability of each variant resulted inversely proportional (Fig. 5A; $R^2 = 0.91$) to cell survival and therefore to the extent of flFNω gene cytotoxicity. These results were confirmed by double staining with acridine orange/ethidium bromide. Control and βgal-lipofected *AlRB*, *AlRA* and *AlRA10* mostly appeared as green-stained healthy cells. After 48 h lipofection with flFNω increased the number of apoptotic/necrotic events as evidenced by the increase of red-stained nuclei (12.4%, 7.2% and 2.9% respectively) compared with control (<1%) (data not shown).

3.4. *flFNω treatments increased ROS production in highly sensitive AlRB*

We have previously described that hIFNβ gene lipofection [30] exerts its cytotoxic effects by increasing ROS production. By means of a H_2DCFDA fluorescence assay, highly sensitive *AlRB* displayed an increase of ROS generation 48 h after flFNω lipofection or incubation with 3000 IU of rflFNω (4-and 2.6-fold respective increase as compared to βgal-lipofected control, Fig. 4C). Meanwhile, *AlRA* and *AlRA10* were not showing a significant ROS increase (n = 4,

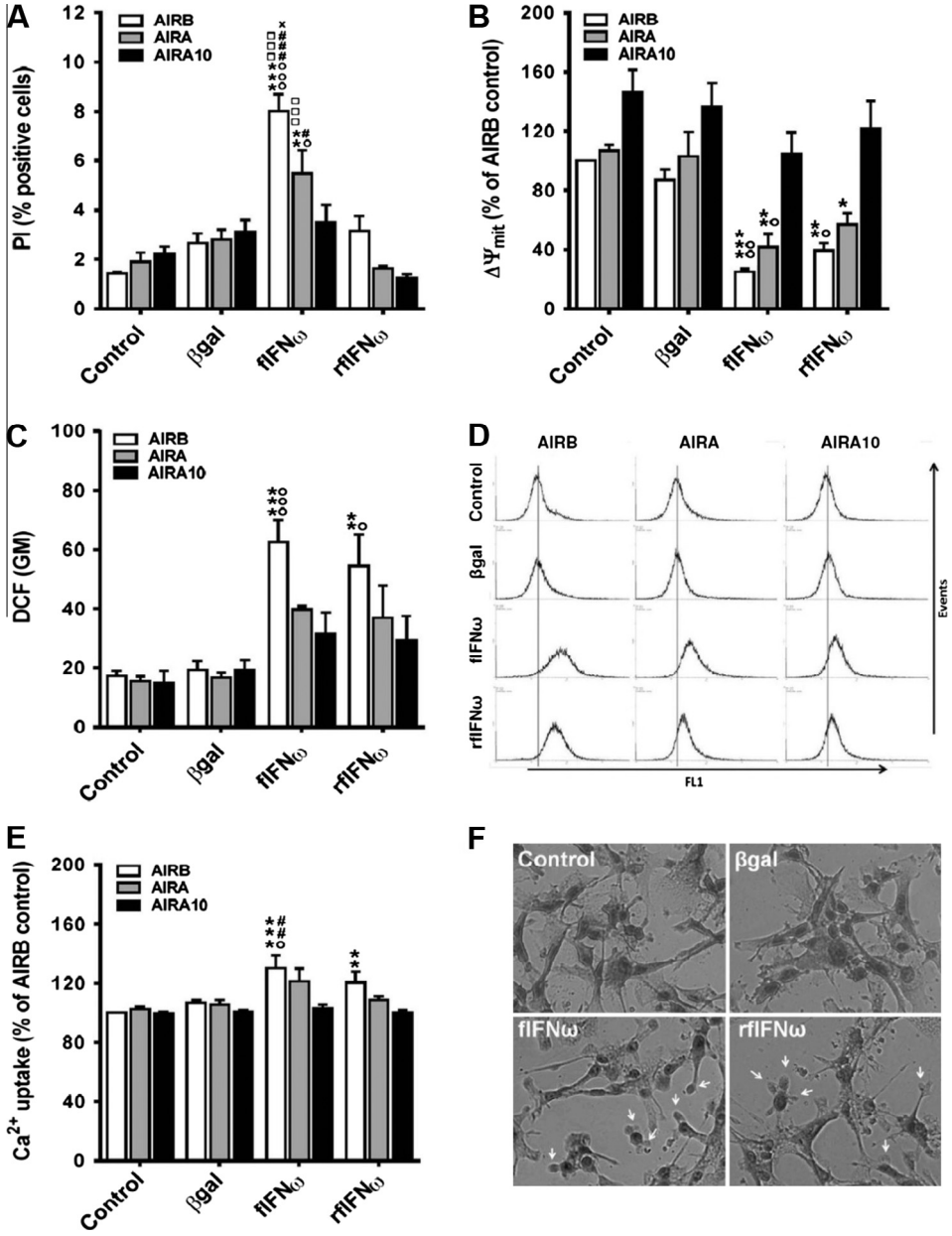

Fig. 4. Mechanisms involved in flNFω action on FMC cells. *AlRB*, *AlRA* and *AlRA10* were lipofected with βgal or flNFω gene or incubated with rflFNω protein (3000 IU/ml). After treatment, non-fixed cell suspensions were incubated with (A) propidium iodide (5 μg/ml), (B) JC-1 (10 μg/ml) or (C and D) H_2DCFDA (0.5 μM) or (E) Fura-2 AM (0.2 μM) and evaluated by flow cytometry as described in Section 2. Results are expressed as means ± s.e.m of at least 4 independent experiments. $^{***}p < 0.001$, $^{**}p < 0.01$ and $^{*}p < 0.05$, with respect to control; $^{\circ\circ\circ}p < 0.001$ and $^{\circ\circ}p < 0.01$ with respect to βgal and $^{\#\#}p < 0.01$ with respect to rflFNω. (F) Representative images of *AlRB* cells showing the blebbing (white arrows) during interferon treatments (200×).

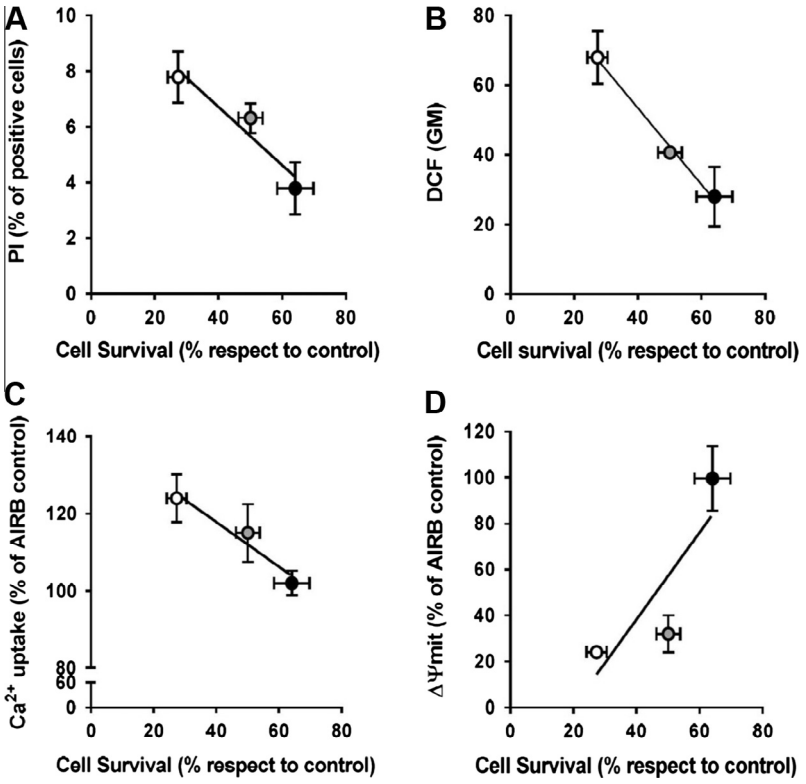

Fig. 5. Correlations among mechanisms, cytotoxicity and FMC cell variants. Cell survivals (X axes) of *AlRB* (white circles), *AlRA* (gray circles) and *AlRA10* (black circles) after 5 days of flFNω gene lipofection are plotted for (A) PI, (B) DCF, (C) Ca^{2+} uptake and (D) changes in mitochondrial membrane potential.

two-way ANOVA) after any of the flFNω treatments. As seen in Fig. 5B, ROS levels correlated with the extent of the cytotoxic response ($R^2 = 0.99$).

3.5. *flFNω treatments disrupted the mitochondrial membrane potential in AlRB and AlRA*

ROS-mediated cytotoxic effects may involve mitochondrial disruption [33]. Therefore, we evaluated whether flFNω treatments could alter the mitochondrial membrane potential (MMP) as detected by the JC-1 fluorescence assay. In untreated cells, the JC-1 probe was mainly in the aggregate state (normal MMP), whereas in *AlRB* and *AlRA*, it was in the monomeric state with both flFNω treatments, thus denoting a loss of MMP (Fig. 4B). On the other hand, the poorly sensitive *AlRA10* presented no loss of MMP either with the flFNω gene or rflFNω protein. Although the disruption of MMP showed no significant correlation with cell survival (Fig. 5D, $R^2 = 0.71$), the most sensitive cell variant presented the most acute loss of MMP.

3.6. *flFNω treatments increased calcium uptake only in the AlRB variant*

AlRB cells treated with both flFNω treatments presented a plasma membrane blebbing (Fig. 4F). These spontaneous protruding blebs have been associated with the generation of resistance against cell injury and depend on calcium uptake [2]. Then, we evaluated the influence of flFNω treatments on the uptake of Ca^{2+} by using Fura-2 AM, a Ca^{2+}-dependent fluorescent probe. After both flFNω treatments sensitive *AlRB* showed a significant increase and *AlRA10* did not present changes in Ca^{2+} uptake, while *AlRA* tended show to slightly increase only after flNFω gene lipofection (Fig. 4E). However, Ca^{2+} uptake correlated with the cytotoxic effect (Fig. 5C; $R^2 = 0.94$).

4. Discussion

As far as we know there is only one previous report about the effects of IFNω gene transfer on growing tumors [5]. Here, we demonstrated for the first time the therapeutic potential of flFNω lipofection on FMC cells. Such therapeutic approach may provide a unique dual advantage in evading the systemic toxicity of the cytokine while improving its potency [8,30]. In the present work, three variants of FMC cells were established and characterized. Subsequently, the antitumor effects of flFNω gene lipofection were compared with those of the recombinant flFNω protein. In agreement with our previous studies with IFNβ [30], flFNω lipofection and expression was equally (*AlRB* and *AlRA*) or more effective (*AlRA10*) than its commercially available analog, the rflFNω protein. Thus, the gene therapy approach emerges as an alternative to treat both sensitive and resistant phenotypes.

Recent studies support the notion that the epithelial to mesenchymal transition (EMT) plays an important role in carcinoma metastasis [29]. A possible explanation for the differences developed by FMC cells during *in vitro* progression may be that at the time of tumor resection, tumor cells had already suffered EMT. Then, *AlRB* cells presented mesenchymal characteristics (high vimentin and low or absent E-cadherin), which, in turn may enhance the ability to migrate and traverse the barriers of endothelial cell junctions. To colonize the metastatic site, cells may reverse (at least in part) the transitory condition by re-expressing adhesion molecules as E-cadherin (*AlRA*, Fig. 1B) or basal-like phenotype-associated proteins as CK5 and αSMA, and decreasing HER2 expression (*AlRA10*, Fig. 1A). These changes support the idea that mesenchymal to epithelial transition (MET) is required for metastatic colonization and also suggest that at least a subgroup of cells of the total population have some potential for plasticity [21]. Furthermore, after reaching passage number 100, we found a complete loss of HER2 expression (data not shown). This variant,

named *AlRATN* due to its triple (*T*) negative (*N*) condition (lack of hormonal receptors and HER2 expression), is under further investigation since it could be an interesting model for a subgroup of tumors that lack molecular target specificity.

Steroid levels have been shown to decrease in feline invasive carcinomas [17,20] during malignant progression [15]. FMC is therefore considered a model to study hormone-independent human breast carcinomas [17,18]. It is interesting to point out that all the established FMC variants appeared as negative for progesterone and estrogen receptor (Fig. 1A).

Taking into account the fact that *AlRA10* was the only variant that successfully formed colonies in soft agar (Fig. 2C), with high proportion of Ki67-positive nuclei and high proliferation rate, we can assume that *AlRA10* was the most aggressive phenotype. In addition, DNA aneuploidy in cell populations, and the amount of cells in S and G2 phases are almost always associated with malignancy [24,32]. In agreement, *AlRA10* presented the highest population in S, G2 and postG2/M compared to *AlRA* and *AlRB*, and this did not change after the treatments. Only 3–5% of *AlRB* cells were positive for Ki67 whereas this percentage increased to >50% in *AlRA10* and *ALRA*. As it was reported [10], the Ki67 nuclear antigen is present in S, G2, and M phases, but absent in G0. Our results suggest that most *AlRB* G0/G1 peak cells are in G0 whereas most *AlRA* and *AlRA10* G0/G1 peak cells are in G1.

The possibility that a long-term exposure to a drug may select tumor cells that become unresponsive and may lead to a more aggressive tumor phenotype, as has been previously proposed for other treatments [12,23] and could account for *AlRA10* resistance to rfIFNω. This issue deserves to be further investigated.

As we have previously described for hIFNβ gene transfer [30], ROS generation during fIFNω treatment seems to be a crucial mechanism for developing antitumor effects since ROS levels were significantly increased in the highly sensitive *AlRB* but not *AlRA* and *AlRA10*. In addition, *AlRA10* maintained the mitochondrial membrane potential during fIFNω gene treatment whereas *AlRA* and *AlRB* significantly diminished it.

In conclusion, our results suggest that fIFNω gene lipofection suppresses cell growth by inducing ROS generation, mitochondrial potential disruption and calcium uptake. It seems that the blockade of this mechanism confers some degree of resistance. Further studies are likely to provide new insights into the relationship between HER2 overexpression, transition proteins and sensitivity to this therapeutic approach. Understanding the biological features of a broader fraction of mammary carcinomas may be helpful to identify means to prevent and treat these carcinomas.

Being FMC a very aggressive disease, the direct cytotoxic effects of fIFNω gene transfer together with the immune and antiangiogenic effects inherent to type I IFNs [14] could settle the basis for the control of tumor growth. The *in vivo* validation of this proposal is compelling.

Disclosure of potential conflict of interest

The authors declare that they have no conflict of interest concerning this article.

Acknowledgments

We thank María D. Riveros and Graciela B. Zenobi for technical advice and assistance. This study was partially supported by grants from ANPCYT/FONCYT (PICT2012-1738) and CONICET (PIP 112 201101 00627). AMT, GCG, LMEF, MSV and MVM are investigators of the Consejo Nacional de Investigaciones Científicas y Técnicas (CONICET, Argentina).

References

[1] A.I. Baba, C. Câtoi, Comparative Oncology, The Publishing House of the Romanian Academy, Bucharest, 2007.
[2] E.B. Babiychuk, K. Monastyrskaya, S. Potez, A. Draeger, Blebbing confers resistance against cell lysis, Cell Death Differ. 18 (2011) 80–89.
[3] F. Belardelli, M. Ferrantini, E. Proietti, J.M. Kirkwood, Interferon-alpha in tumor immunity and immunotherapy, Cytokine Growth Factor Rev. 13 (2002) 119–134.
[4] G.P. Burrai, S.I. Mohammed, M.A. Miller, V. Marras, S. Pirino, M.F. Addis, S. Uzzau, E. Antuofermo, Spontaneous feline mammary intraepithelial lesions as a model for human estrogen receptor- and progesterone receptor-negative breast lesions, BMC Cancer 10 (2010) 156.
[5] P.F. Chen, G.F. Fu, H.Y. Zhang, G.X. Xu, Y.Y. Hou, Liposomal plasmid DNA encoding human thymosin alpha and interferon omega potently inhibits liver tumor growth in ICR mice, J. Gastroenterol. Hepatol. 21 (2006) 1538–1543.
[6] J.C. Cheng, C. Klausen, P.C. Leung, Hydrogen peroxide mediates EGF-induced down-regulation of E-Cadherin expression via p38 MAPK and snail in human ovarian cancer cells, Mol. Endocrinol. 24 (2010) 1569–1580.
[7] R. De Maria, M. Olivero, S. Iussich, M. Nakaichi, T. Murata, B. Biolatti, M.F. Di Renzo, Spontaneous feline mammary carcinoma is a model of HER2 overexpressing poor prognosis human breast cancer, Cancer Res. 65 (2005) 907–912.
[8] L.M. Finocchiaro, C. Fondello, M.L. Gil-Cardeza, Ú.A. Rossi, M.S. Villaverde, M.D. Riveros, G.C. Glikin, Cytokine-enhanced vaccine and interferon-β plus suicide gene therapy as surgery adjuvant treatments for spontaneous canine melanoma, Hum. Gene Ther. 26 (2015) 367–376.
[9] J. Friedrich, C. Seidel, R. Ebner, L.A. Kunz-Schughart, Spheroid-based drug screen: considerations and practical approach, Nat. Protoc. 4 (2009) 309–324.
[10] J. Gerdes, H. Lemke, H. Baisch, H.H. Wacker, U. Schwab, H. Stein, Cell cycle analysis of a cell proliferation-associated human nuclear antigen defined by the monoclonal antibody Ki-67, J. Immunol. 133 (1984) 1710–1715.
[11] G.C. Glikin, L.M. Finocchiaro, Clinical trials of immunogene therapy for spontaneous tumors in companion animals, Sci. World J. 2014 (2014) 718520.
[12] J.L. Hsieh, C.S. Lu, C.L. Huang, G.S. Shieh, B.H. Su, Y.C. Su, C.H. Lee, M.Y. Chang, C. L. Wu, A.L. Shiau, Acquisition of an enhanced aggressive phenotype in human lung cancer cells selected by suboptimal doses of cisplatin following cell deattachment and reattachment, Cancer Lett. 321 (2012) 36–44.
[13] K. Hughes, J.M. Dobson, Prognostic histopathological and molecular markers in feline mammary neoplasia, Vet. J. 194 (2012) 19–26.
[14] E. Jonasch, F.G. Haluska, Interferon in oncological practice: review of interferon biology, clinical applications, and toxicities, Oncologist 6 (2001) 34–55.
[15] S.E. Lana, G.R. Rutteman, S.J. Withrow, Tumors of the mammary gland, in: S.J. Withrow, D.M. Vail (Eds.), Withrow & MacEwen's Small Animal Clinical Oncology, Saunders, St. Louis, 2007, pp. 619–636.
[16] J.Y. Manesh, R. Shafiee, B. Pedram, H.Z. Malayeri, S. Mohajer, S. Ahmadi, S. Ahmadi, J. Javanbakht, A. Mokarizadeh, F. Khadivar, Improving the diagnosis, treatment, and biology patterns of feline mammary intraepithelial lesions: a potential model for human breast masses with evidence from epidemiologic and cytohistopathologic studies, Tumour Biol. 35 (2014) 12109–12117.
[17] J. Martín de las Mulas, M. Van Niel, Y. Millán, J. Ordás, M.A. Blankenstein, F. Van Mil, W. Misdorp, Progesterone receptors in normal, dysplastic and tumourous feline mammary glands. Comparison with oestrogen receptors status, Res. Vet. Sci. 72 (2002) 153–161.
[18] P.M. Martin, M. Cotard, J.P. Mialot, F. André, J.P. Raynaud, Animal models for hormone-dependent human breast cancer. Relationship between steroid receptor profiles in canine and feline mammary tumors and survival rate, Cancer Chemother. Pharmacol. 12 (1984) 13–17.
[19] F. Millanta, M. Calandrella, S. Citi, D. Della Santa, P. Poli, Overexpression of HER-2 in feline invasive mammary carcinomas: an immunohistochemical survey and evaluation of its prognostic potential, Vet. Pathol. 42 (2005) 30–34.
[20] F. Millanta, M. Calandrella, I. Vannozzi, A. Poli, Steroid hormone receptors in normal, dysplastic and neoplastic feline mammary tissues and their prognostic significance, Vet. Rec. 158 (2006) 821–824.
[21] O.H. Ocaña, R. Córcoles, A. Fabra, G. Moreno-Bueno, H. Acloque, S. Vega, A. Barrallo-Gimeno, A. Cano, M.A. Nieto, Metastatic colonization requires the repression of the epithelial-mesenchymal transition inducer Prrx1, Cancer Cell 22 (2012) 709–724.
[22] C. Penzo, M. Ross, R. Muirhead, R. Else, D.J. Argyle, Effect of recombinant feline interferon-omega alone and in combination with chemotherapeutic agents on putative tumour-initiating cells and daughter cells derived from canine and feline mammary tumours, Vet. Comp. Oncol. 7 (2009) 222–229.
[23] A.O. Pisco, S. Huang, Non-genetic cancer cell plasticity and therapy-induced stemness in tumour relapse: 'what does not kill me strengthens me', Br. J. Cancer 112 (2015) 1725–1732.
[24] T.A. Potapova, J. Zhu, R. Li, Aneuploidy and chromosomal instability: a vicious cycle driving cellular evolution and cancer genome chaos, Cancer Metastasis Rev. 32 (2013) 377–389.
[25] Ú.A. Rossi, M.L. Gil-Cardeza, M.S. Villaverde, L.M. Finocchiaro, G.C. Glikin, Interferon-β gene transfer induces a strong cytotoxic bystander effect on melanoma cells, Biomed. Pharmacother. 72 (2015) 44–51.
[26] S. Santos, E. Bastos, C.S. Baptista, D. Sá, C. Caloustian, H. Guedes-Pinto, F. Gärtner, I.G. Gut, R. Chaves, Sequence variants and haplotype analysis of cat ERBB2 gene: a survey on spontaneous cat mammary neoplastic and nonneoplastic lesions, Int. J. Mol. Sci. 13 (2012) 2783–2800.

[27] A.M. Targovnik, M.S. Villaverde, M.B. Arregui, M. Fogar, O. Taboga, G.C. Glikin, L.M.E. Finocchiaro, O. Cascone, M.V. Miranda, Expression and purification of recombinant feline interferon in the baculovirus-insect larvae system, Process Biochem. 49 (2014) 917–926.
[28] S. Tateyama, B.P. Priosoeryanto, R. Yamaguchi, K. Uchida, K. Ogiwara, A.T. Suchiya, In vitro growth inhibition activities of recombinant feline interferon on all lines derived from canine tumours, Res. Vet. Sci. 59 (1995) 275–277.
[29] J.P. Thiery, H. Acloque, R.Y. Huang, M.A. Nieto, Epithelial-mesenchymal transitions in development and disease, Cell 139 (2009) 871–890.
[30] M.S. Villaverde, M.L. Gil-Cardeza, G.C. Glikin, L.M. Finocchiaro, Interferon-β lipofection II. Mechanisms involved in cell death and bystander effect induced by cationic lipid-mediated interferon-β gene transfer to human tumor cells, Cancer Gene Ther. 19 (2012) 420–430.
[31] D.A. Wiese, T. Thaiwong, V. Yuzbasiyan-Gurkan, M. Kiupel, Feline mammary basal-like adenocarcinomas: a potential model for human triple-negative breast cancer (TNBC) with basal-like subtype, BMC Cancer 13 (2013) 403.
[32] T. Zatoński, T. Krecicki, D. Duś, M. Zalesska-Krecicka, M. Jeleń, M. Kaczmarz, S +G2M phase fraction and index of DNA in the aneuploid laryngeal cancer, Otolaryngol. Pol. 58 (2004) 321–326.
[33] G. Zheng, J. Lyu, J. Huang, D. Xiang, M. Xie, Q. Zeng, Experimental treatments for mitochondrial dysfunction in sepsis: a narrative review, J. Res. Med. Sci. 20 (2015) 185–195.
[34] L. Zitvogel, L. Galluzzi, O. Kepp, M.J. Smyth, G. Kroemer, Type I interferons in anticancer immunity, Nat. Rev. Immunol. 15 (2015) 405–414.